

ORIGINAL RESEARCH ARTICLE

Imbalance of gut *Bacteroides* and *Prevotella* contributes to memory decline in ovariectomized mice fed with high-fat diet

Lu Zeng[†], Xiaobin An[†], Wentao Xu, Jing Ma, Yang Qu, Guitian Cong, Meijie Chen, Yan Wu, Xuqiao Wang, Jinan Yang, and Jing Ai*

Department of Pharmacology (The State-Province Key Laboratories of Biomedicine-Pharmaceutics of China), College of Pharmacy of Harbin Medical University, Harbin, Heilongjiang, China

Abstract

The rates of incidence and progression of Alzheimer's disease (AD) vary significantly among post-menopausal women. However, the mechanisms that underlie this phenomenon remain obscure. Here, we established the high-fat diet-fed ovariectomized (OVXHF) mouse model and observed significant memory deficits in this model. Using 16S rDNA sequencing, we found that OVXHF mice displayed higher biodiversity and a distinct gut microbiome composition compared with normal chow-fed mice. Functional analysis further revealed that genes associated with the iron complex transport system and ATP-binding cassette are differentially expressed in OVXHF mice. Moreover, normal fecal microbiota transplantation (FMT) successfully restored the cognitive impairments in OVXHF mice through rebalancing the gut microbiota. In particular, the *Bacteroides*-to-*Prevotella* ratio was significantly increased in OVXHF mice but rescued by FMT. Altogether, these results suggest that an imbalance between *Bacteroides* and *Prevotella* in the gut microbiota accelerates the process of cognitive dysfunction in postmenopausal women on a high-fat diet.

Keywords: Estrogen deficiency; High-fat diet; Cognition decline; Gut microbiome; *Bacteroides-Prevotella* imbalance

[†]These authors contributed equally to this work.

***Corresponding author:**

Jing Ai
(aijing@ems.hrbmu.edu.cn)

Citation: Zeng L, An X, Xu W, *et al.* Imbalance of gut *Bacteroides* and *Prevotella* contributes to memory decline in ovariectomized mice fed with high-fat diet. *Adv Neurol.* 2026;5(1):93-110.
doi: 10.36922/AN025200055

Received: May 12, 2025

1st revised: August 14, 2025

2nd revised: August 27, 2025

Accepted: August 28, 2025

Published online: September 17, 2025

Copyright: © 2025 Author(s). This is an Open-Access article distributed under the terms of the Creative Commons Attribution License, permitting distribution, and reproduction in any medium, provided the original work is properly cited.

Publisher's Note: AccScience Publishing remains neutral with regard to jurisdictional claims in published maps and institutional affiliations.

1. Introduction

Dementia is a pathological neurodegenerative disorder characterized by a progressive decline in cognition. Alzheimer's disease (AD) accounts for 60–80% of all dementia cases, making it the predominant neurodegenerative cause of the condition.^{1,2} Increasing evidence suggests that AD affects men and women unequally. It has been reported that after the age of 65, 5.8 million Americans are diagnosed with AD, including 3.6 million women and 2.2 million men.³ These findings suggest that sex differences matter in the development of AD. One potential explanation for the increased susceptibility of women to AD is menopause, which causes a drastic decline in estrogen levels. Estrogens (including estrone, estradiol, and estriol) are a group of neuroactive steroid hormones related to memory and cognition.⁴ As expected, estrogen deprivation of women after menopause can increase the risk of AD, according to a 3-year longitudinal study.⁵ Accordingly, studies have found that estrogen hormone replacement therapy can have a protective effect against cognitive decline.^{6–8} However, other evidence also shows that

hormone replacement therapy has no benefit in AD, with some cases even indicate a negative effect on cognition.^{9,10} Considering the fact that estrogen supplementation fails to consistently relieve AD symptoms and not all aged women develop AD, we wondered whether there were other risk factors underlying the high morbidity of AD in female.

In light of the multifactorial origin of dementia, mounting evidence suggests that lifestyle factors significantly contribute to its progression.¹¹ Lately, the connection between diet and brain function has become a major focus of research. The Mediterranean diet (MD), which is characterized by high portion of whole grains, veggies, nuts, beans, and olive oil, moderate amount of fish, and limited portion of dairy and meat,¹² is widely considered a major boon to overall health. Extensive research indicates a correlation between adherence to MD and a reduced risk of AD, as well as enhanced cognitive abilities.¹³⁻¹⁵ Conversely, a high-fat Western dietary pattern may hasten cognitive impairment.^{16,17} Therefore, this raises the question: what distinguishes MD from the Western diet, and how do these differences exert opposite effects on dementia? One of the most noteworthy features of MD is its low-fat content. Therefore, we speculated that a high-fat diet (HFD) may be a contributory factor accelerating cognitive decline in postmenopausal women.

With the rapid development and evolution of new technologies, the microbiota residing in the gastrointestinal tract has been increasingly regarded as the “second brain” that regulates host health.^{18,19} The gut-brain axis, a concept proposed by researchers, describes a bidirectional communication between gut microbiota and the brain, facilitated through the sympathetic and parasympathetic nervous systems, as well as circulating neuro-modulatory molecules and bacterial metabolites.^{20,21} Moreover, the microbiome is highly adaptable and susceptible to change due to a range of environmental and host-specific triggers. When it comes to these influencers, dietary habits stand out as the main driver in shaping both the composition and operational aspects of the microbiome.²² HFD has been associated with an increased abundance in lipopolysaccharide (LPS)-expressing bacteria, resulting in higher LPS levels in both human²³ and mice circulation.²⁴ Furthermore, lard-rich diet can increase the abundance of *Bacteroides*, *Turicibacter*, and *Bilophila* spp., promoting white adipose tissue inflammation and insulin insensitivity.²⁵ However, it remains unknown how HFD in combination with estrogen deficiency affects gut microbiota and cognitive functions.

To explore the role of HFD in facilitating estrogen deficiency-induced cognition impairment, we established an ovariectomized (OVX) mouse model fed with HFD to mimic the situation of postmenopausal women adopting

a fat-enriched diet. We then examined the effect of OVX and HFD on the intestinal microbiota. We found that HFD accelerated cognitive decline in OVX mice. Moreover, 16S rDNA sequencing facilitated a comparative analysis of gut microbiota composition and profiles across groups. Finally, we also examined whether normal fecal microbiota transplantation could reverse the cognitive impairment and gut microbiota structure of HFD-fed OVX mice.

2. Materials and methods

2.1. Mice and diet

Juvenile female C57BL/6 mice were obtained from the Animal Center of the Second Affiliated Hospital of Harbin Medical University. Mice were housed in a temperature-controlled room at 25°C under a 12 h light/dark cycle and had ad libitum access to food and water. Under specific pathogen-free conditions, all mice were maintained in a climate chamber with controlled light and humidity (4 mice/chamber), supplied with HEPA-filtered air, and provided with irradiated food and water. The mice were fed either a regular chow diet or an HFD, which consisted of 45% of calories from fat, 35% from carbohydrates, and 20% from protein (HFK Bioscience, #H10045). Body weight was measured weekly. After 8 weeks of feeding, the mice were subjected to behavioral tests or fecal collection. All animal experiments were approved by the Institutional Animal Care and Use Committee of Harbin Medical University and the Institute of Laboratory Animal Science of China. All procedures conformed to the Directive 2010/63/EU of the European Parliament.

2.2. OVX surgery

Two-month-old female mice were anesthetized using an intraperitoneal injection of sodium pentobarbital (100 mg/kg). After prepping the surgical site, we shaved the fur from the flank region, specifically the area nestled between the last rib and just above the pelvis. The skin was then disinfected with chlorhexidine solution before making an incision along the dorsal midline. The muscle layers were carefully separated with curved-tip scissors, and the ovarian fat pad was gently exteriorized through the opening. Hemostatic tweezers were used to firmly clamp the region just below the ovary, and the area to be removed was tied off with two knots using sterile thread, effectively demarcating the surgical field. Following this, the ovary was excised. The same procedure was then replicated on the left side. Following the procedure, the abdominal incision was closed using stainless steel wound clips. The animals were kept under observation in the laboratory until they had fully come around from the anesthesia. After that, they were returned to the animal care facilities and checked on a daily basis.

2.3. Barnes-Maze test

Behavioral assessments using the Barnes maze were conducted following established protocols with minor adjustments.²⁶ In a nutshell, the mice were subjected to evaluations during the day's light phase, and they were moved into the behavioral testing area an hour ahead of the experiment's kickoff. The Barnes maze featured a clear, elevated, well-lit white circular platform, measuring 91 cm across, and it had 20 evenly spaced, 5 cm wide holes around the edge, with one of those leading to a secret exit. The walls of the testing area were adorned with spatial cues featuring unique patterns and forms. The assessment was broken down into phases of habituation, learning, and the probe test. In the experimental setup, a 500-lux light and an electric fan were employed to generate light, air currents, and noise—key elements to trigger escape responses. On the day of habituation, the research mouse spent 30 seconds acclimatizing to the target box, before being positioned in the center of the apparatus. It was then allowed to roam until it discovered the escape tunnel or the 200-s test session was reached. The acquisition phase entailed a total of 5 days of daily training sessions, with two rounds of trials each day (with a time cap of 3 min per trial; approximately an hour between trials), and the starting point was shuffled among the four quadrants. Each trial began with the mouse placed in a start chamber situated in the middle of one of the quadrants. A 15-s countdown was initiated, and following its conclusion, the start chamber was raised, unleashing the mouse to navigate the maze. The trial comes to a close either when the mouse makes a beeline for the escape tunnel or when the clock strikes 3 min. Should the mouse be unable to locate the escape tunnel within the 3-min window, the researcher will assist it and let it chill in the tunnel for 15 s. Post-trial, the maze and escape tunnel are sanitized with a 75% ethanol solution. Throughout the training phase, the mouse's path, errors, and time taken to locate the target hole were meticulously documented using a video tracking software called SuperMaze (Shanghai XinRuan Software, China). Three days after the final training session, the probe trial takes place, where the escape box is eliminated, and the start chamber is centered in the apparatus. The subject mouse was permitted to locate the target hole within a 3-min window, with the response latency and errors for finding the target hole recorded.

2.4. Novel object recognition test

In accordance with the previously outlined methodology,²⁷⁻²⁹ novel object recognition tests (ORTs) were conducted. Before the acclimatization phase, the mice were permitted to roam freely in an open field to become acclimated.

Following this, on the day after the habituation period, the mice were given the opportunity to freely investigate two indistinguishable objects—a pair of Lego bricks, 12.5 cm tall, 2.5 cm deep, and 7.5 cm wide, constructed from alternating hues of blue, yellow, red, and green—positioned at predetermined spots within the testing area for a duration of 10 min. To track the duration of exploration for each object, the SuperMaze video-tracking system, developed by XinRuan in Shanghai, China and utilizing nose-point detection technology, was employed. Investigative engagement was defined as olfactory or tactile interaction with an object when the mouse's nose was within 2 cm of the item. At the end of each session, the mice were gently returned to their familiar habitats, and the testing chamber, along with all objects was meticulously sanitized with 75% ethanol solution, followed by a thorough air-drying process for a duration of 3 min. After a 24-h intersession interval (ISI) without intervention, one of the familiar objects was swapped out for a new one—a tissue culture flask that stood at 15.5 cm tall, 3.5 cm deep, and 9 cm across. The following formula was used to determine object preference: Preference percentage = (Time to investigate the particular object/total exploration time for both objects) × 100%. If the overall exploration time was <10 s, the data were not included.

2.5. Fecal microbiota transplantation

Fecal microbiota transplantation was performed as previously described.³⁰ To deplete native gut microorganisms, OVXHF mice were given 0.2 mL/mouse of triple antibiotics (1.25 mg/L vancomycin, 2.5 mg/L ampicillin, and 2.5 mg/L metronidazole) every day for three consecutive days before transplantation. Then, 200 mg of stool (from Sham mice) was reconstituted in 5 mL of PBS, vortexed for 3 min, and allowed to settle by gravity for 2 min. A 200 μ L of the supernatant was then administered to recipient mice by oral gavage to accomplish the transplant. FMT was conducted on OVXHF mice once daily for 30 consecutive days through oral gavage 1 month after OVX surgery and HFD exposure.

2.6. Gut microbiota DNA extraction

Fecal DNA was extracted using the QIAamp DNA Stool Mini Kit (Qiagen). Approximately 200 mg of mouse fecal sample was mixed with 1 ml of EX Inhibition Buffer and the proper quantity of glass beads (Qiagen) with a 0.5 mm diameter. After that, the sample was homogenized by vortex-mixing twice a minute at 60 Hz. The following procedures were applied to the supernatant after it had been treated with an InhibitEX Tablet. A NanoDrop 2000 spectrophotometer (Thermo Scientific, MA, USA) was used to measure the amount of DNA.

2.7. 16S rDNA gene sequencing

A universal primer targeting the conserved region of 16S rDNA was constructed as follows: 5'-CCTACGGGRRSGCAGCAG-3' (universal primer 341F) and 5'-GGACTACVVGTTATCTAATC-3' (universal primer 806R) for PCR amplification of the variable region (V3+V4) of the rRNA gene or specific gene fragments. The PCR products were analyzed using the Illumina NovaSeq PE250 system (Illumina, Inc., CA, United States).

2.8. Gut microbiota taxonomical and functional annotation

After sifting through the raw data and removing reads with over 10 substandard bases (those less than Q20) or 15 adapter sequence bases, clean reads were processed in QIIME2 for taxonomic annotation. Operational taxonomic units (OTUs) were clustered at 97% sequence similarity using UPARSE. Functional prediction of microbial communities was performed with PICRUSt2 (v2.3.0) based on ASV data and taxonomic information, yielding KEGG Orthology (KO) pathway distributions for each sample. To measure the alpha diversity across the samples, we used Mothur (v.1.30) and its suite of tools such as the Rarefaction curve, Shannon index, Rank abundance curve, Chao1 richness estimator, and the Simpson diversity index. Beta diversity was analyzed using unweighted UniFrac bandwagon, followed by principal component analysis (PCA), principal coordinates analysis (PCoA), and unweighted pair-group method with arithmetic mean (UPGMA) clustering. Finally, linear discriminant analysis effect size (LEfSe) was applied to assess the impact of the intestinal microbiome.

2.9. Statistical analysis

The results were presented as mean \pm standard error of mean. A Student's *t*-test was applied for statistical comparisons between two groups, whereas a one-way analysis of variance was utilized to assess differences across three or more groups. Tukey's *post hoc* tests were conducted to delve into the significant main effects. Findings were deemed statistically significant when $p < 0.05$.

3. Results

3.1. HFD facilitated episodic and spatial memory impairment in OVX mice

To investigate whether HFD could predispose estrogen-deficient mice to cognitive impairment, we subjected female mice to HFD following ovariectomy (OVX) surgery. Previous studies have shown that HFD is always accompanied by overweight and serum lipid disturbances.³¹ Interestingly, after 1 month of HFD, we

found no differences in body weight or serum lipid levels in any group (Figure 1A-D). Analogous to the above results, there were no differences in latency and error times in the Barnes maze or discrimination index in novel ORT in each group (Figure 1E-R). The above result indicates that there is no episodic and spatial memory impairment after 1 month of HFD in OVX mice.

Even after 2 months of HFD, there was still no differences in body weight and serum lipid levels, including total triglyceride (TG) and total cholesterol (TC), in the Sham+HFD group (Figure 2A-D). However, these parameters were significantly increased in 2-month OVXHF mice, indicating that HFD could affect the body weight and serum lipid levels of estrogen-deficient mice (Figure 2A-D). We also found that 2-month OVXHF mice displayed significantly impaired spatial memory, manifested as extended total distance (Figure 2E-G), prolonged escape latency (Figure 2H and I), and more errors (Figure 2J and K) during probe trial of the Barnes maze test. Notably, no significant difference of average speed was found among the four groups (Figure 2L). As for novel object recognition (NOR), OVXHF mice showed decreased exploration frequency (Figure 2N), time spent with the novel object (Figure 2Q), and a lower discrimination index (Figure 2O-R) on day 2, reflecting attenuated episodic memory. Together, these results showed that HFD could facilitate the episodic and spatial memory impairment in OVX mice.

3.2. HFD induces gut dysbiosis in OVX mice

HFD has been reported to alter the intestinal microbiome and induce cognitive decline through the gut-brain axis.^{32,33} To investigate whether HFD induces specific changes in the gut microbial population in OVX mice, we conducted 16S rDNA sequencing to characterize the gut microbiota (GM) under different conditions. After size and quality screening, as well as chimera elimination, we got the sequence length distribution histogram so that optimized sequences for accurate analysis can be obtained (Figure 3A). OTUs were clustered at 97% sequence similarity using Usearch,³⁴ and 117 OTUs were identified as the core microbiome across all samples (Figure 3B). PCA revealed significant clustering of microbiota across groups (Figure 3C). Although the Sham+HFD and OVX groups showed significant difference in the first and second principal components, respectively (PCA1: 15.91%, PCA2: 9.53%) when compared to Sham group, the two experimental groups were found to be on par with one another, while they markedly differed from OVXHF group. These results indicated that the HFD caused significant changes on GM in OVX mice.

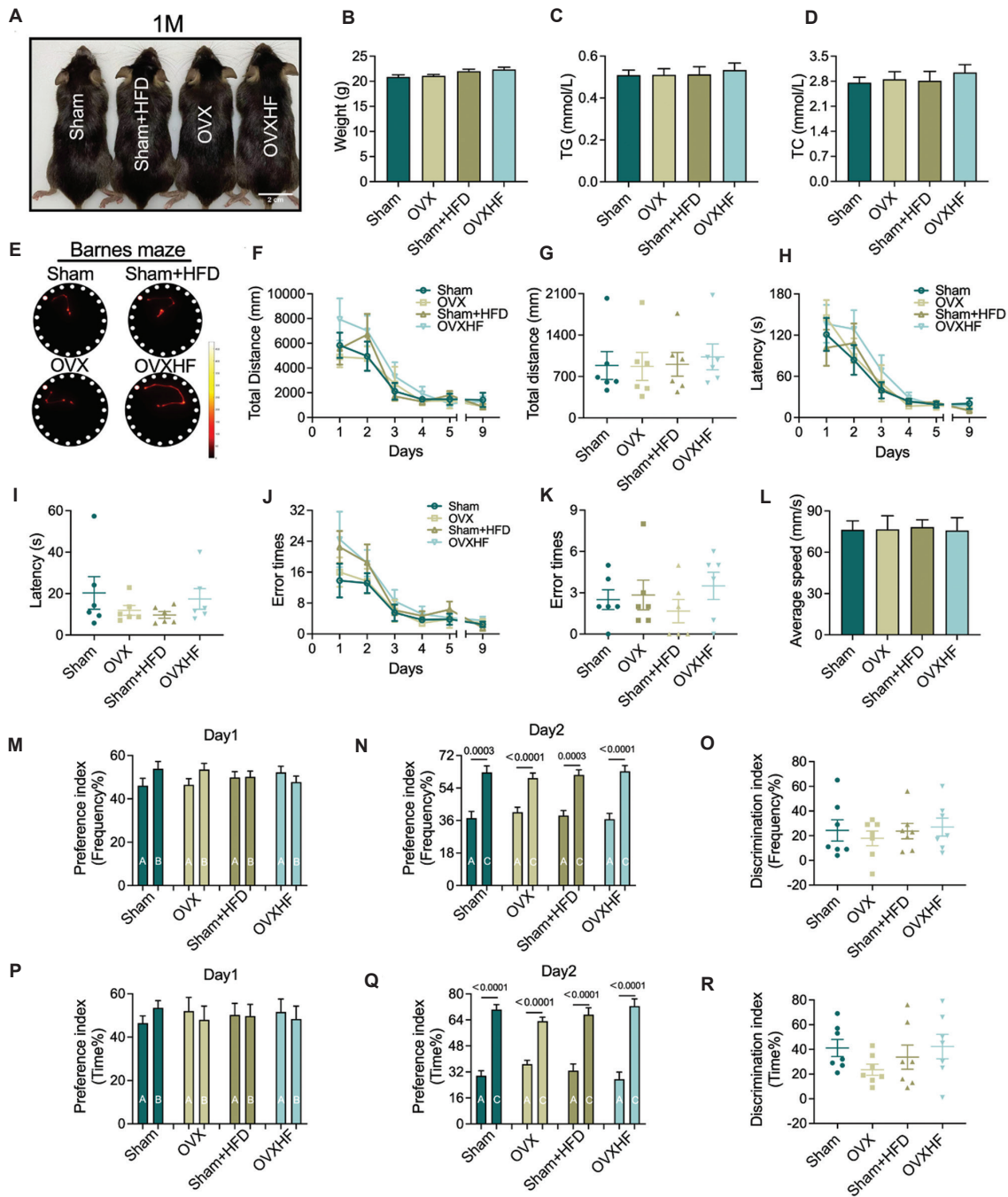


Figure 1. One-month HFD failed to cause cognitive decline in OVX mice. (A) Comparison of the body shape of 1-month (1M) Sham, Sham+HFD, OVX, and OVXHF mice. (B) Body weight at the 4th week for Sham (*n* = 9), OVX (*n* = 8), Sham+HFD (*n* = 8), OVXHF (*n* = 9). (C) The levels of total glycerol in serum of 1M Sham (*n* = 6), OVX (*n* = 6), Sham+HFD (*n* = 6), OVXHF (*n* = 6). (D) The levels of total cholesterol in the serum of the above four groups. (E) Schematic diagram of the traces in the Barnes maze test during the probe trial. (F) Total distance during the Barnes maze test for 1M Sham (*n* = 6), 1M OVX (*n* = 6), 1M Sham+HFD (*n* = 6), 1M OVXHF (*n* = 6). (G) Total distance of the four groups in the Barnes maze during the probe trial. (H) Escape latency during the Barnes maze test of these four groups. (I) Escape latency of the four groups in the Barnes maze during the probe trial. (J) Number of errors in the Barnes maze test. (K) Number of errors in the Barnes maze test during the probe trial. (L) Average moving speed of the four groups during the Barnes maze test. (M) Preference index for frequency on day 1 of 1M Sham (*n* = 8), OVX (*n* = 8), Sham+HFD (*n* = 8), OVXHF (*n* = 8) in the ORT. (N) Preference index for frequency on day 2 of the above four groups. (O) Discrimination index for the frequency of the four groups. (P) Preference index for contact time on day 1 of the four groups. (Q) Preference index for contact time on day 2 of the four groups. (R) Discrimination index for contact time of the four groups. Data are presented as mean ± SEM and analyzed by one-way ANOVA.

Abbreviations: ANOVA: Analysis of variance; 1 M: 1-month; HFD: High-fat diet; ORT: Object recognition test; OVX: Ovariectomized; OVXHF: HFD-fed OVX; SEM: Standard error of the mean.

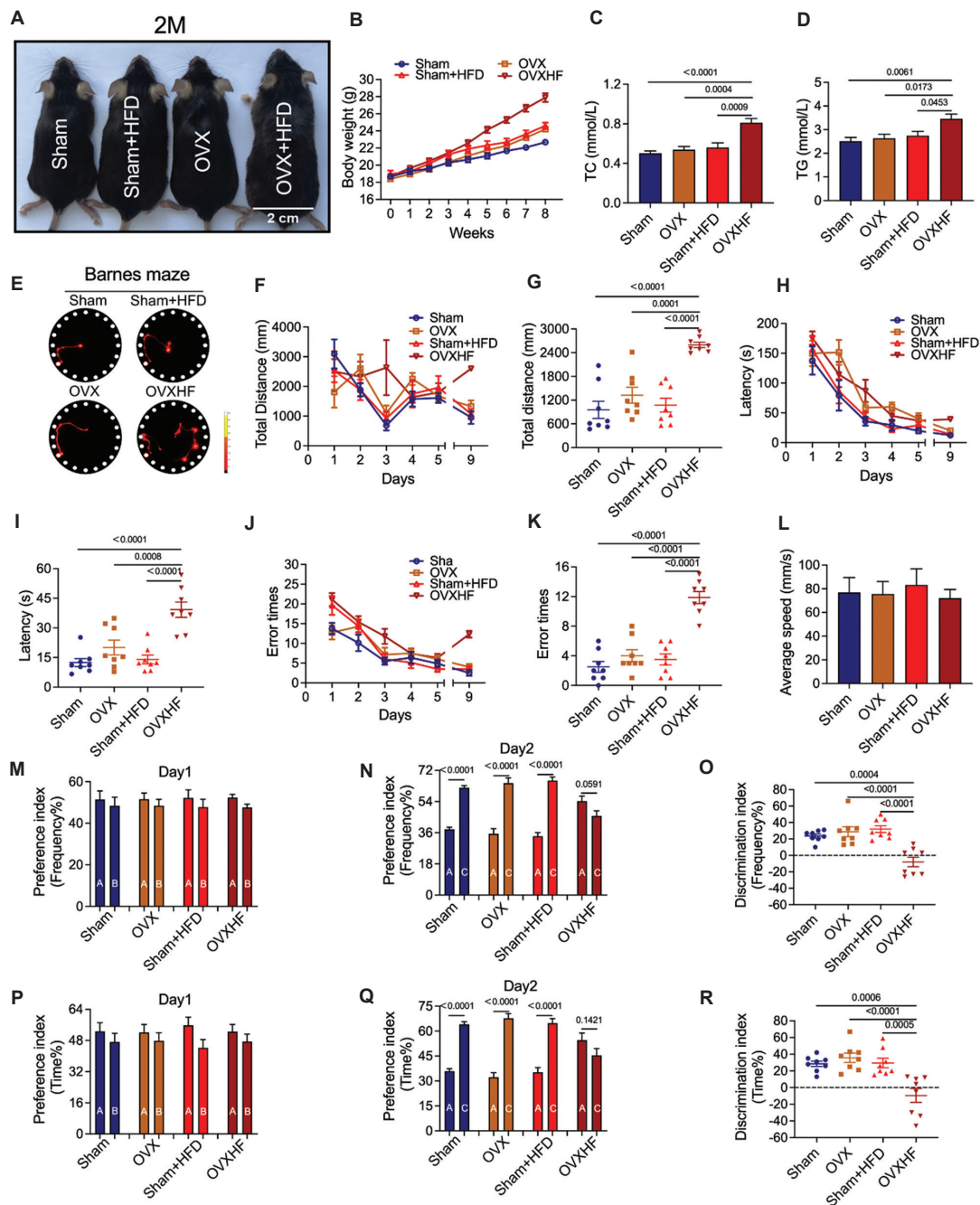


Figure 2. Two-month HFD facilitated cognitive impairment in OVX mice. (A) Comparison of the body shape of 2-month (2M) Sham, Sham+HFD, OVX, and OVXHF mice. (B) Weekly body weight of Sham ($n = 9$), OVX ($n = 8$), Sham+HFD ($n = 8$), OVXHF ($n = 9$) mice. (C) The levels of total cholesterol in the serum of 2M Sham, OVX, Sham+HFD, and OVXHF ($n = 6$ for each group). (D) The levels of total glycerol in the serum of the above four groups. (E) Schematic diagram of the traces in the Barnes maze test during the probe trial. (F) Total distance during the Barnes maze test for each group ($n = 8$). (G) Total distance of the four groups in the Barnes maze during the probe trial. (H) Escape latency during the Barnes maze test of the four groups. (I) Escape latency during the Barnes maze test of the four groups. (J) Number of errors in the Barnes maze test. (K) Number of errors in the Barnes maze test during the probe trial. (L) Average moving speed of the four groups during the Barnes maze test. (M) Preference index for frequency on day 1 of 2M Sham ($n = 8$), OVX ($n = 8$), Sham+HFD ($n = 8$), OVXHF ($n = 8$) mice in the ORT. (N) Preference index for frequency on day 2 of the above four groups. (O) Discrimination index for the frequency of the four groups. (P) Preference index for contact time on day 1 of the four groups. (Q) Preference index for contact time on day 2 of the four groups. (R) Discrimination index for contact time of the four groups. Data are presented as mean \pm SEM and analyzed by one-way ANOVA.

Abbreviations: ANOVA: Analysis of variance; HFD: High-fat diet; ORT: Object recognition test; OVX: Ovariectomized; OVXHF: HFD-fed OVX; SEM: Standard error of the mean; 2M: 2 months.

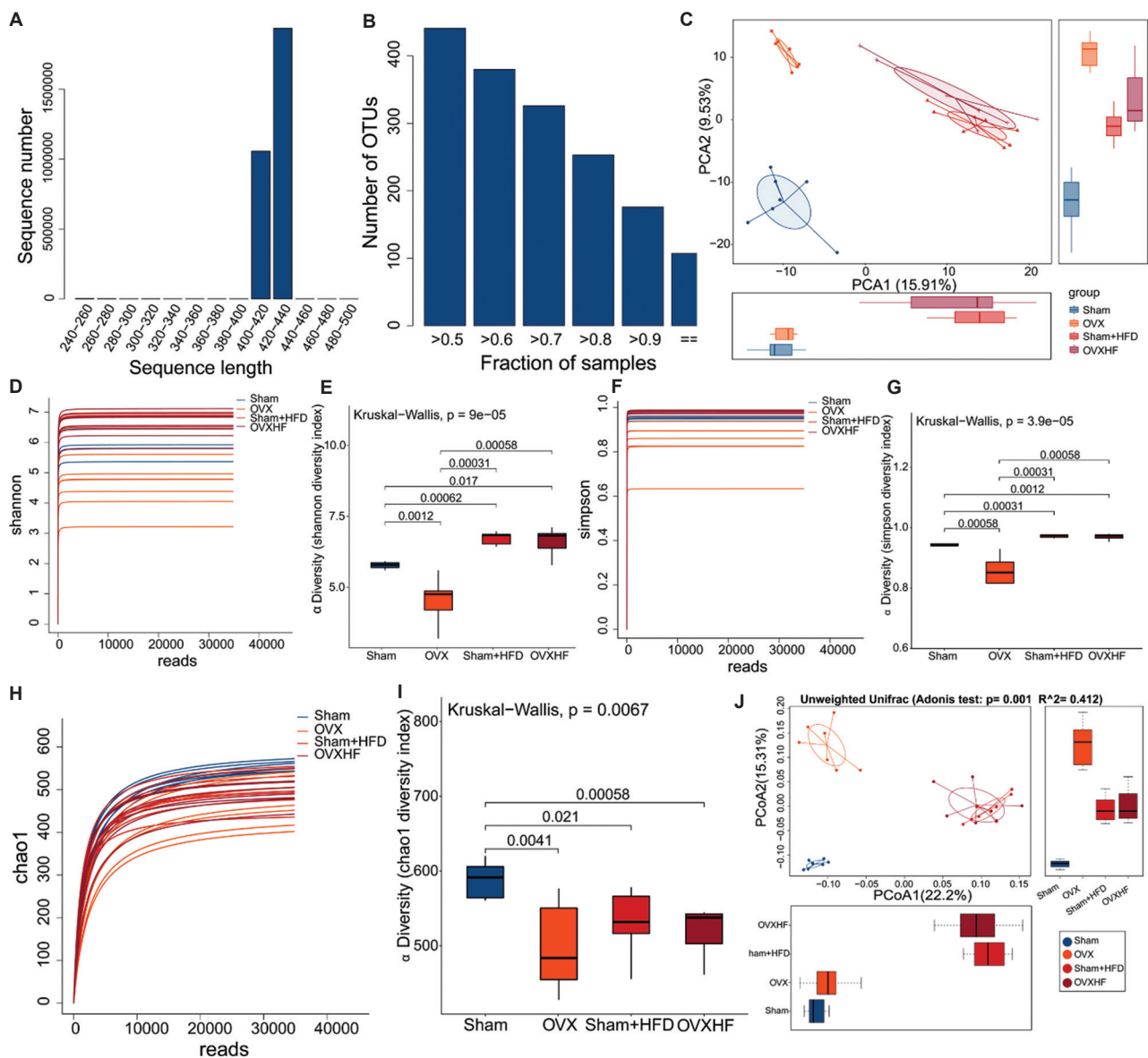


Figure 3. HFD altered the alpha and beta diversities of gut microbiota in OVX mice. (A) The sequence length distribution histogram of 16S rDNA sequencing. (B) Core microbiome that covers 100% samples. (C) Principal component analysis (PCA) of the microbiota composition in 2-month Sham ($n = 7$), OVX ($n = 7$), Sham+HFD ($n = 8$), and OVXHF ($n = 7$) mice. (D–G) Shannon and Simpson indices of 16S rDNA sequencing indicated community diversity in the four groups. (H–I) Chao1 index of 16S rDNA sequencing shows community richness in the above four groups. (J) Principal coordinates analysis (PCoA) based on unweighted UniFrac analysis of the Adonis test shows beta-diversity of these four groups. Each symbol represents a single fecal sample. Data are presented as mean \pm SEM and analyzed by one-way ANOVA.

Abbreviations: HFD: High-fat diet; OVX: Ovariectomized; OVXHF: HFD-fed OVX; SEM: Standard error of the mean; ANOVA: Analysis of variance.

Alpha diversity reflects both sample diversity, represented by indices like Shannon and Simpson, and species richness, such as Chao1.³⁵ Compared to the Sham group, Shannon and Simpson indices were significantly reduced in the OVX-only group. However, in the OVXHF mice, these indices bounced back, mirroring the levels seen in the Sham+HFD group. This suggests that HFD reshapes gut bacterial diversity in OVX mice, counteracting the

diversity loss caused by estrogen deficiency (Figure 3D–G). The Chao1 indices were significantly decreased in the Sham+HFD, OVX, and OVXHF groups compared to the Sham group, but there were no significant differences among them. This indicates that both HFD and OVX can decrease gut bacterial richness; however, HFD does not affect the gut bacterial richness in OVX mice (Figure 3H and I). PCoA of Aitchison distances further

revealed significantly altered GM composition in OVX, Sham+HFD, and OVXHF groups compared to the Sham control, while the Sham+HFD and OVXHF groups were of similar composition (Figure 3J). Accordingly, these results suggest that HFD can change the GM composition and induce GM dysbiosis in OVX mice.

3.3. The ratio of *Bacteroides/Prevotella* increased in OVXHF mice

To further clarify the effects of HFD and estrogen depletion on intestinal flora at the genus level, bacterial makeup was examined thoroughly. LEfSe analysis was used to present the bacteria that played an important role in Sham, OVX, Sham+HFD, and OVXHF mice (Figure 4A). Bar plots presented a comprehensive breakdown of the prevalence of various genera across the 29 fecal samples, with *Alloprevotella*, *Prevotella*, *Lactobacillus*, *Clostridium XIVaI*, and *Bacteroides* dominating in the four groups (Figure 4B). Then, we analyzed the explicit alterations of these bacterial genus, respectively. In total, we identified 6 genera significantly changed in Sham+HFD, OVX, or OVXHF mice, respectively (Figure 4C-H). Notably, *Alloprevotella* abundance was increased in OVX mice compared to the Sham group but significantly reduced in both Sham+HFD and OVXHF mice (Figure 4C). *Streptococcus* was the only genus consistently decreased in all three groups (Figure 4D). The level of *Turicibacter* and *Bifidobacterium* was both elevated in OVXHF mice but not OVX and Sham+HFD mice (Figure 4E and F). The relative prevalence of *Prevotella* in OVX and OVXHF mice mirrored that of *Alloprevotella*, while stayed unchanged in Sham+HFD mice (Figure 4G). The level of *Bacteroides* was significantly upregulated in Sham+HFD and OVXHF mice (Figure 4H). This study indicates that the human gut microbiota can be categorized into three distinct enterotypes, primarily characterized by *Bacteroides*, *Prevotella*, or *Clostridiales* organisms.³⁶ Thus, we wondered whether the ratio of *Bacteroides/Prevotella* (B/P) was associated with the cognitive impairment caused by HFD and OVX co-exposure. OVX alone failed to cause disturbance on the B/P ratio while HFD slightly increased this ratio (Figure 4I). Interestingly, the combination of HFD with OVX led to dramatic elevation of the B/P ratio (Figure 4I). In conclusion, HFD reshaped the microbial spectrum in OVX mice, and the rise of B/P ratio may represent a key microbial signature associated with cognitive impairment under combined HFD and estrogen deficiency.

3.4. Microbial functional alterations in the OVXHF mice

After dissecting the bacterial composition across groups, we further explored the enrichment of KO functions in

OVXHF mice. By comparing the 16S rDNA gene sequences against genomic reference databases, the functional potential of the microbial community was predicted. LEfSe analysis was employed to assess the impact of KO genes from each group on the differential outcomes and to identify corresponding KO genes responsible for notable differential effects (Figure 5A). Among these, only the ATP-binding cassette (ABC)-2 type transport system permease protein was increased in OVX, Sham+HFD, and OVXHF group versus Sham group (Figure 5B). Subfamily B of the ABC proteins showed a modest rise in the OVX cohort versus the Sham, whereas HFD induced a notable drop in the ABC subfamily B levels in OVX mice (Figure 5C). Furthermore, genes belong to the iron complex transport system, RNA polymerase sigma-70 factor, and 3-oxoacyl- [acyl-carrier protein] reductase were remarkably decreased in OVX group in contrast to Sham group (Figure 5D-G, K). Comparatively, expression of these genes demonstrates a reverse pattern in the OVXHF cohort relative to OVX mice (Figure 5D-G, K). In addition, the abundance of cold shock protein, methyl-accepting chemotaxis protein, and 2,3-biphosphoglycerate-dependent phosphoglycerate showed no obvious difference between Sham and OVX group, but HFD separately increased or decreased the abundance of these genes in the OVX group (Figure 5H-J). Taken together, the results suggest that HFD causes disturbance in the functional structure of GM in OVX mice which may account for the cognitive impairment induced by HFD.

In addition, we investigated the association between bacterial genera and host physiological or behavioral parameters. LEfSe correlation analysis revealed that the weight of mice was positively correlated with *Elusimicrobium*, *Blautia*, and *Christensenella* but negatively correlated with *Odoribacter*, *Mycoplasma*, *Clostridium XVIII*, *Sporobacter*, and *Paraprevotella*. Barnes maze errors showed positive associations with *Desulfovibrio* and *Turicibacter* but inversely correlated with *Prevotella*, *Alloprevotella*, and *Streptococcus*. We also identified the genera that are closely correlated with the levels of 5-hydroxytryptamine (5-HT), L-Kynurenine (L-KYN) and L-Tryptophan (L-TRP), which are indispensable nutrients for the hosts (Figure 5L).

3.5. Fecal microbiota transplantation restored cognitive impairment in OVXHF mice

Our findings demonstrate that HFD accelerates memory decline in OVX mice while disrupting both the composition and functional capacity of the gut microbiota. However, it is still not clear whether these gut imbalances are the culprit behind the cognitive decline. To address this, we introduced healthy murine gut microbiota into

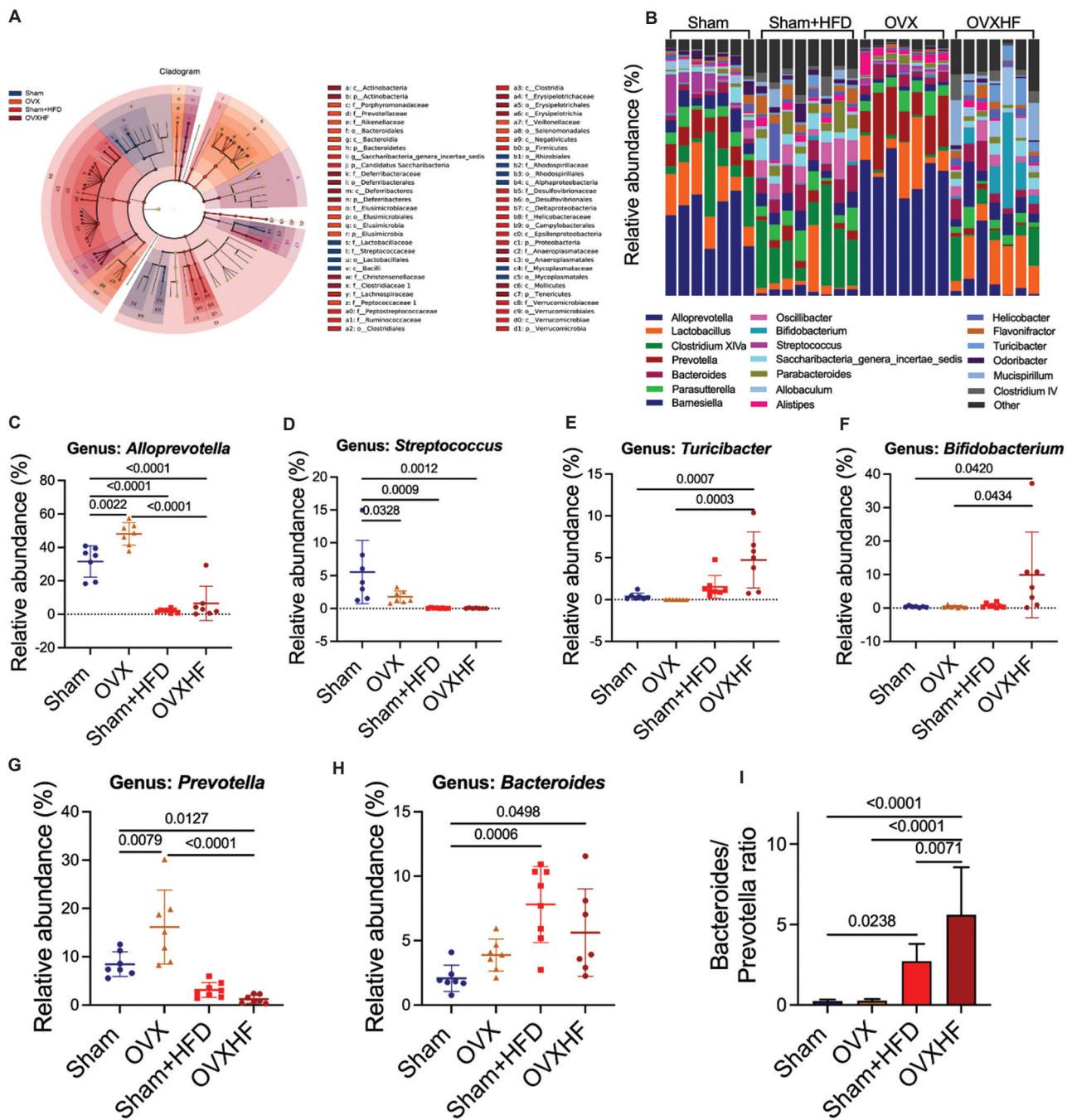


Figure 4. Characterization of gut microbiota composition at the genus level. (A) Linear discriminant analysis (LDA) effect size (LefSe) analysis showing the bacteria that played an important role in 2-month Sham ($n = 7$), OVX ($n = 7$), Sham+HFD ($n = 8$), and OVXHF ($n = 7$) mice. (B) Proportions of different bacterial genus in the gut microbiota of the above four groups. Each column represents one mouse sample. (C–H) The bacterial genus that were dysregulated by OVX and HFD, including *Alloprevotella*, *Prevotella*, *Streptococcus*, *Bacteroides*, *Turicibacter*, and *Bifidobacterium*. (I) The ratio of *Bacteroides* and *Prevotella* in the four groups. Data are presented as mean \pm SEM and analyzed by one-way ANOVA. Abbreviations: ANOVA: Analysis of variance; HFD: High-fat diet; OVX: Ovariectomized; OVXHF: HFD-fed OVX; SEM: Standard error of the mean.

the digestive systems of OVXHF mice through oral administration. FMT alleviated weight gain and serum TC and TG levels in OVXHF mice (Figure 6A–D). Moreover, the Barnes maze task showed that OVXHF mice

receiving FMT exhibited markedly improved path length, latency, and error times in locating the escape aperture (Figure 6E–L). In ORT study, FMT notably augmented OVXHF mice interaction duration and rate with the novel

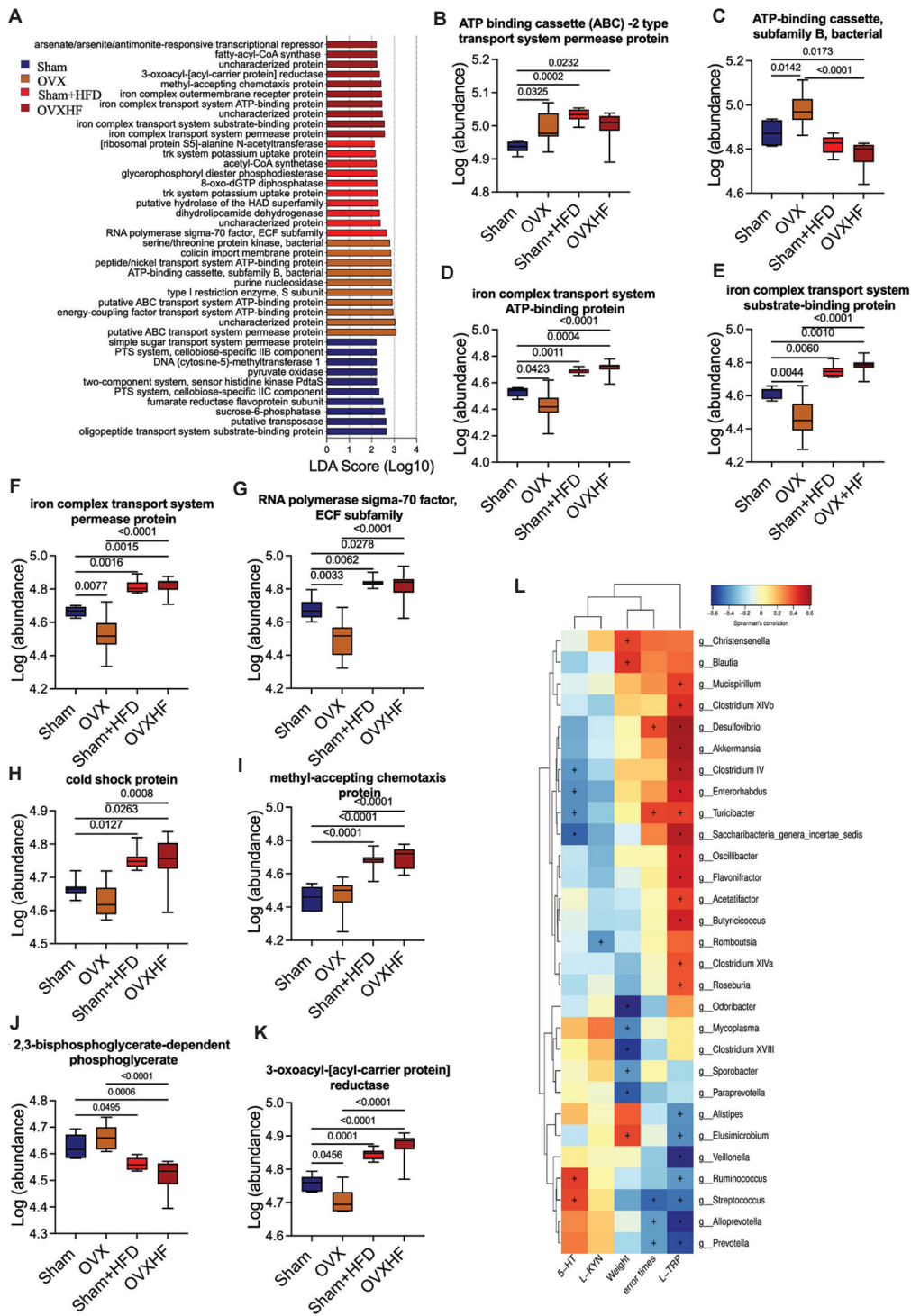


Figure 5. KEGG ortholog functional analysis of gut microbiota in Sham, OVX, Sham+HFD, and OVXHF mice. (A) LefSe analysis was used to find the counterpart KEGG ortholog (KO) genes that produce significant differential effects (default screening criteria LDA >2). The ordinate represents the log value obtained by LDA for KO genes with a significant effect in the 2-month Sham, OVX, Sham+HFD, and OVXHF groups. (B–K) The KO genes that were dramatically altered by OVX and HFD in Sham ($n = 7$), OVX ($n = 7$), Sham+HFD ($n = 8$), and OVXHF ($n = 7$) mice. (L) LefSe analysis revealed the correlation of various genera with body weight, error times, 5-HT, L-KYN, and L-TRP levels. Data are presented as mean \pm SEM and analyzed by one-way ANOVA. * $p < 0.05$; ** $p < 0.01$.

Abbreviations: ANOVA: Analysis of variance; HFD: High-fat diet; LDA: Linear discriminant analysis; LefSe: LDA effect size; OVX: Ovariectomized; OVXHF: HFD-fed OVX; SEM: Standard error of the mean.

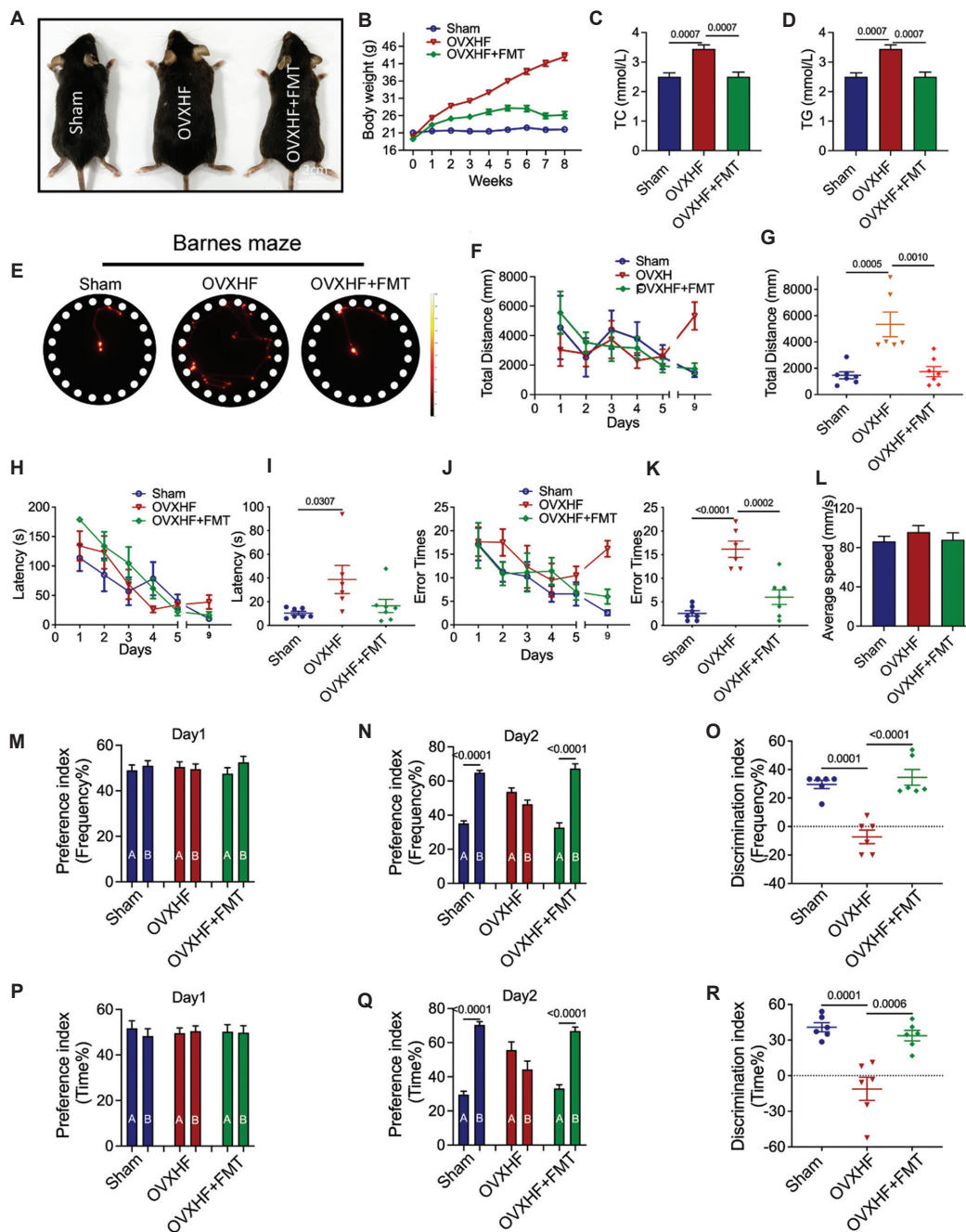


Figure 6. Fecal microbiota transplantation restored the spatial and episodic memory impairment of OVXHF mice. (A) Comparison of the body shape of 2M Sham, OVXHF, and OVXHF+FMT mice. (B) Weekly body weight of Sham ($n = 7$), OVXHF ($n = 6$), and OVXHF+FMT ($n = 7$) mice. (C) The levels of total cholesterol in the serum of 2-month Sham, OVXHF, and OVXHF+FMT mice. $n = 6$ for each group. (D) The levels of total glycerol in the serum of the above four groups. (E) Schematic diagram of the traces in the Barnes maze test during the probe trial. (F) Total distance during the Barnes maze test for Sham ($n = 7$), OVXHF ($n = 6$), and OVXHF+FMT ($n = 7$) mice. (G) Total distance of the four groups in the Barnes maze during the probe trial. (H) Escape latency during the Barnes maze test of these four groups. (I) Escape latency during the Barnes maze test of these four groups. (J) Number of errors in the Barnes maze test. (K) Number of errors in the Barnes maze test during the probe trial. (L) Average moving speed of the four groups during the Barnes maze test. (M) Preference index for frequency on day 1 of 2M Sham, OVXHF, and OVXHF+FMT mice. $n = 6$ for each group. (N) Preference index for frequency on day 2 of the above four groups. (O) Discrimination index for frequency of the four groups. (P) Preference index for contact time on day 1 of the four groups. (Q) Preference index for contact time on day 2 of the four groups. (R) Discrimination index for contact time of the four groups. Data are presented as mean \pm SEM and analyzed by one-way ANOVA.

Abbreviations: ANOVA: Analysis of variance; FMT: Fecal microbiota transplantation; OVXHF: High-fat diet-fed ovariectomized mice; SEM: Standard error of the mean; 2M: 2 months.

item, along with elevating the novelty preference score (Figure 6M-R). Together, these results indicate that FMT can reverse the obesity phenotype and spatial and episodic memory impairments in OVXHF mice. Concurrently, our study supports the notion that HFD exacerbates cognitive decline in OVX mice through intestinal dysbiosis.

3.6. Fecal microbiota transplantation restored intestinal bacterial structure in OVXHF mice

To further investigate whether the beneficial effects of FMT on cognitive function in OVXHF mice were linked to the altered functional structure of their gut microbiota, we re-employed 16S rDNA sequencing to pinpoint the specific shifts in gut microbiota following FMT. First, goods coverage indicated that the sequencing exhibits excellent coverage (Figure 7A). The Shannon and Simpson indices were increased in OVXHF and FMT-treated OVXHF mice than in Sham mice, but no significant difference was observed between the two groups (Figure 7B-C). However, the Chao1 index was reduced in OVXHF mice, whereas FMT application dramatically increased the Chao1 index in OVXHF mice (Figure 7D). These results indicated that FMT significantly restored the richness of OVXHF mice. Analysis on the genus level constructure showed that microbial composition in OVXHF mice was altered after FMT administration (Figure 7E). Then, we further analyzed the abundance of these bacterial genus and identified 7 genera that changed by FMT. In particular, FMT restored the abundance of *Prevotella* and *Parabacteroides* in OVXHF, while increasing the abundance of *Bacteroides*, *Oscillibacter*, *Alistipes*, and *Flavonifractor* (Figure 7F). In accordance with the restoration of cognitive impairment by FMT, the B/P ratio was significantly decreased in the OVXHF mice supplied with normal gut flora (Figure 7G), further supporting its role in the cognition decline caused by HFD and estrogen deficiency.

Similarly, we also performed the KO functional analysis in FMT-treated OVXHF mice. The results indicated that the level of ABC, putative ABC transport system permease protein, and 2,3-biphosphoglycerate mutase was restored by FMT administration (Figure 8A-C). In addition, genes related to ABC transport system, peptide/nickel transport system, and Lacl family transcriptional regulator were markedly enriched in FMT-treated OVXHF mice (Figure 8D-I). Taken together, these functional genes might be associated with the amelioration of cognitive impairment caused by OVXHF.

4. Discussion

Clinical evidence shows that not all women experience rapid cognitive decline during menopause, though the underlying reasons remain unclear. Dietary patterns affect

the cognitive process,³⁷ and it is speculated that different diet may participate in the process of rapid cognitive decline in menopausal women. In this study, we found that HFD could accelerate cognitive impairment in 2-month OVX mice rather than 1-month OVX mice. Moreover, 16S rDNA sequencing revealed considerable shifts in both the makeup and operation of the gut microbiota in 2-month OVXHF mice. Importantly, FMT effectively restored microbial balance and reversed cognitive decline in these OVXHF mice. Particularly, an increase in *Bacteroides/Prevotella* (B/P) ratio may account for the cognitive impairment in OVXHF mice. The findings clearly indicate that the HFD is a critical risk factor for AD in post-menopausal women, suggesting that early dietary interventions could be a potential strategy to prevent cognitive deterioration in perimenopausal women.

The greater incidence of AD among females compared to males has sparked significant concern.³⁸ Previous studies have focused on the fluctuation of estrogen levels after menopause and they actually identified a close relation between AD and estrogen deficiency.³⁹ However, not all women experience cognition decline after menopause, and the disease initiation varies among individuals. Moreover, our previous study found that female mice developed episodic memory impairment after 3 months of estrogen deficiency and spatial memory decline after 5 months of estrogen deficiency,⁴⁰ suggesting that additional risk factors may contribute to cognitive deterioration in postmenopausal females. HFD, an unhealthy dietary habit, has been found to exert a more severe effect in female AD mice rather than male AD mice.⁴¹ Thus, we hypothesized that HFD might be a potential risk factor accelerating cognitive impairment in postmenopausal females. However, in this study, 1-month HFD failed to induce cognitive impairment in OVX mice. Instead, after 2-month HFD, OVX mice showed impaired spatial and episodic memory, indicating that 2-month HFD could expedite the cognitive decline in OVX mice. Considering these findings, maintaining a healthy diet may help mitigate cognitive decline after menopause.

Although estrogen levels decline sharply during menopause in women compared to the gradual reduction of testosterone in age-matched men,⁴² the abrupt loss of estrogen after OVX still cannot perfectly simulate natural menopause process concomitant with exaggerate physiological and behavioral effects. In addition, other ovarian hormones such as testosterone may also be depleted after OVX, which serves as another defect of this model.⁴³ Thus, our future plan will continue to study the mechanism of cognitive impairment in perimenopausal women using the natural aging mouse model.

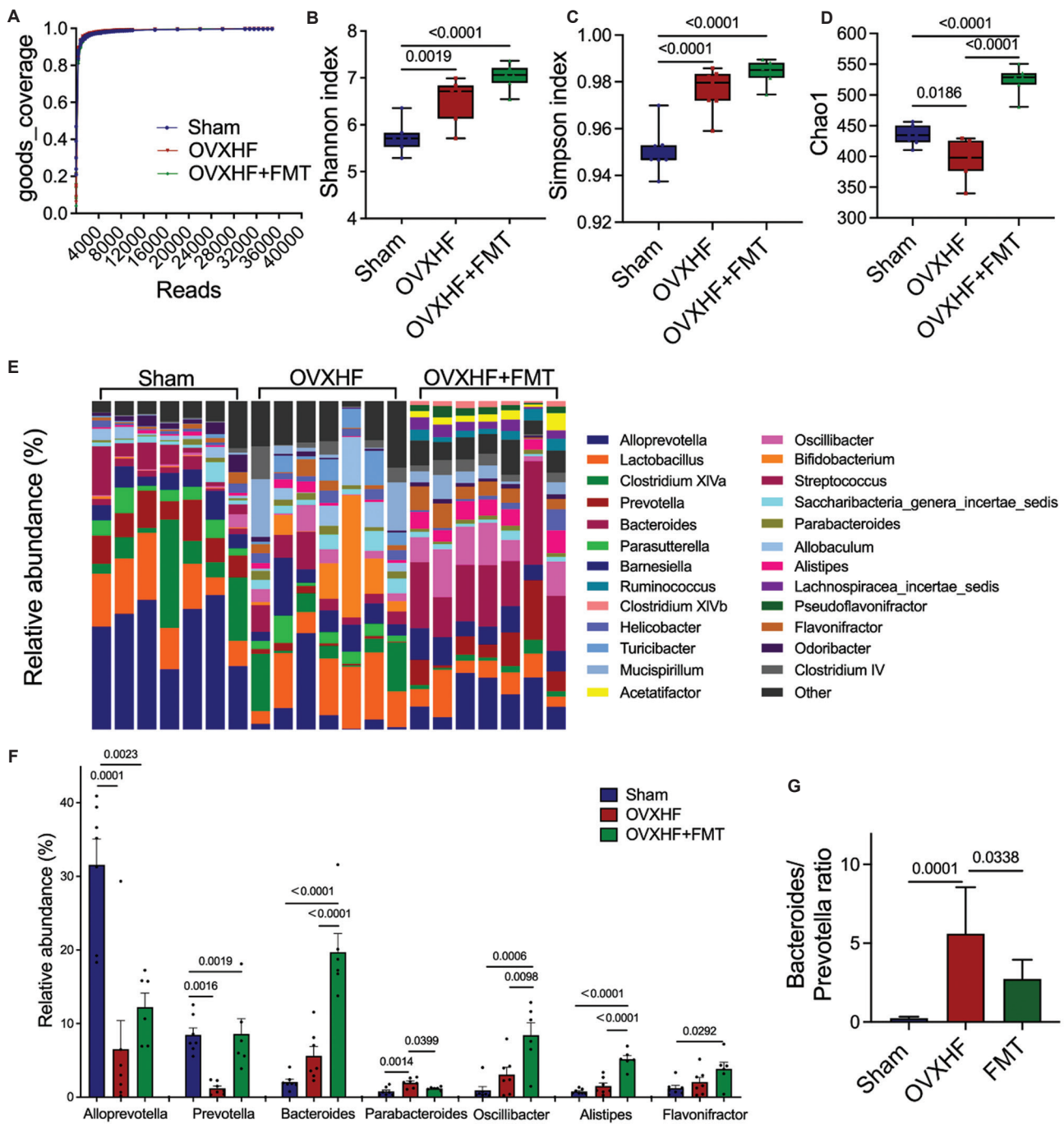


Figure 7. Gut bacteria alterations after fecal microbiota transplantation in OVXHF mice. (A) The goods coverage index of 16S rDNA sequencing. (B–D) Alpha diversity represented by Shannon, Simpson, and Chao1 indices of 16S rDNA sequencing for 2-month Sham ($n = 7$), OVXHF ($n = 7$), and OVXHF+FMT ($n = 7$) mice. (E) Proportional abundance of gut microbiota from the above three groups at the genus level. Each column indicates one mouse sample. (F) The bacterial genus which relative abundance was rectified after FMT, including *Alloprevotella*, *Prevotella*, *Bacteroides*, *Parabacteroides*, *Oscillibacter*, *Alistipes*, and *Flavonifractor*. (G) The *Bacteroides/Prevotella* ratio in the Sham ($n = 7$), OVXHF ($n = 7$), and OVXHF+FMT ($n = 6$) mice. Data are presented as mean \pm SEM and analyzed by one-way ANOVA.

Abbreviations: ANOVA: Analysis of variance; FMT: Fecal microbiota transplantation; OVXHF: High-fat diet-fed ovariectomized mice; SEM: Standard error of the mean.

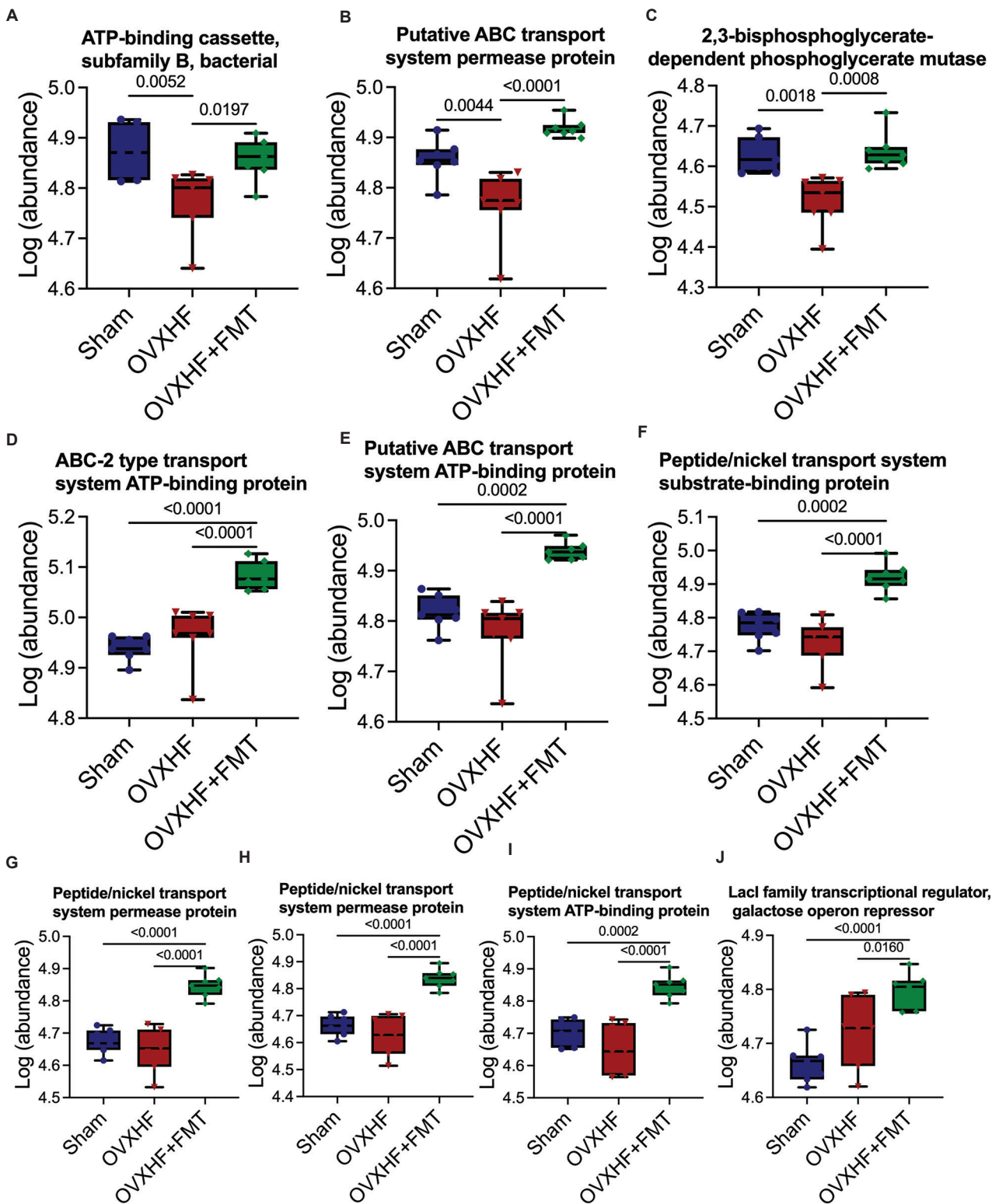


Figure 8. KEGG ortholog functional analysis of gut microbiota in Sham, OVXHF, and OVXHF+FMT mice. (A–C) The abundance of ATP-binding cassette, subfamily B, putative ABC transport system permease protein, and 2,3-bisphosphoglycerate-dependent phosphoglycerate mutase was restored after FMT in OVXHF mice. *n* = 7 for each group. (D–J) FMT significantly increased the abundance of the ABC transport system family, peptide/nickel transport system family, and LacI family transcriptional regulator, galactose operon repressor. Data are presented as mean ± SEM and analyzed by one-way ANOVA. Abbreviations: ANOVA: Analysis of variance; FMT: Fecal microbiota transplantation; OVXHF: High-fat diet-fed ovariectomized mice; SEM: Standard error of the mean.

In recent years, GM and its role in neurodegenerative diseases have attracted considerable attention.⁴⁴ HFD can effectively affect GM composition and increase the risk of AD.⁴⁵ However, whether and how HFD could bring about gut dysbiosis in OVX mice remains unclear. In this study, we profiled the gut microbiome of OVXHF mice through 16S rDNA sequencing techniques and identified 6 genera that exhibited notable shifts among which the abundance of *Prevotella* was dramatically increased in OVX mice while decreased in Sham+HFD and OVXHF mice. Studies have discovered an inverse relationship between *Prevotella* and cognitive impairment.⁴⁶ *Bacteroides* is a probiotic that provides the host with volatile fatty acids serving as an energy source.⁴⁷ This study revealed a heightened prevalence of *Bacteroides* in Sham+HFD and OVXHF groups, a finding that appears inconsistent with some earlier findings. However, *Prevotella*- and *Bacteroides*-dominated gut flora have been identified as two major enterotypes of human which are closely associated with diet patterns.³⁶ Thereinto, the *Bacteroides*-dominated enterotype mainly appears in people with high-fat/high-sugar “Western” diet, whereas the *Prevotella*-dominant enterotype is found in people possessing a fiber-rich plant-based diet pattern.^{48,49} In this study, the B/P proportion within the gut microbiota of mice was analyzed, revealing a moderate rise in the HFD group and a marked increase in the OVXHF group. Furthermore, normal gut microbiota transplantation successfully restored the B/P ratio. Our findings align with previous studies and suggest that a balance between *Bacteroides* and *Prevotella* is essential for maintaining host neuropsychiatric health.

Beyond genus-level changes, differential genera were correlated with environmental factors. We found that *Prevotella*, *Alloprevotella*, and *Streptococcus* were negatively correlated with error times in the Barnes maze, implying these genera might account for the spatial memory impairment of OVXHF mice. Tryptophan, or TRP, is an essential amino acid, in which imbalances in TRP's metabolic process play a significant role in the advancement of certain neurological disorders, including depression, AD, and glioma.⁵⁰ Here, we examined links between intestinal bacteria and L-TRP, along with its downstream products 5-HT and L-KYN. *Prevotella*, *Alloprevotella*, and *Streptococcus* were negatively correlated with L-TRP, while *Streptococcus* alone was positively correlated with 5-HT. These results suggest that these three genera may participate in the pathological process of cognitive deficit through disruption of TRP metabolism.

Closer examination of the results revealed that the variation trends of GM were surprisingly consistent in the Sham+HFD and OVXHF mice but different from

that in OVX mice, suggesting that HFD exerts a stronger influence on GM than estrogen deficiency. However, even though the Sham+HFD and OVXHF mice shared similar characteristics of GM, Sham+HFD mice failed to develop cognitive impairment. This might be attributed to the complexity of the GM composition and the absence of estrogen deficiency which could also cause lipid and glucose metabolic disorders.⁵¹ Thus, HFD alone was insufficient to induce cognitive decline, whereas co-exposure with estrogen deficiency led to pronounced spatial and episodic memory impairments. The interaction between HFD and estrogen deficiency on host physiology is complicated and interesting, warranting further investigation.

5. Conclusion

Taken together, HFD serves as a critical risk factor that facilitates cognitive decline in post-menopausal women through gut dysbiosis. Normal fecal microbiota transplantation effectively restored the cognitive function caused by HFD and estrogen deficiency, with the imbalance between *Bacteroides* and *Prevotella* likely playing a pivotal role. Thus, further studies should focus on elucidating the underlying mechanisms linking this imbalance in cognitive function and exploring the feasibility of GM-based therapeutic approaches for AD.

Acknowledgments

None.

Funding

This work was funded by the National Science and Technology Innovation 2030—Major Program of “Brain Science and Brain-Like Research” (2022ZD0211804 to J, A.).

Conflict of interest

Jing Ai is an Editorial Board Member of this journal but was not in any way involved in the editorial and peer-review process conducted for this paper, directly or indirectly. Separately, other authors declared that they have no known competing financial interests or personal relationships that could have influenced the work reported in this paper.

Author contributions

Conceptualization: Jing Ai, Lu Zeng, Xiaobin An

Formal analysis: Lu Zeng, Xiaobin An

Investigation: Lu Zeng, Xiaobin An, Jing Ma, Guitian Cong, Meijie Chen, Yang Qu, Yan Wu, Xuqiao Wang, Jinan Yang

Methodology: Lu Zeng, Xiaobin An, Wentao Xu, Jing Ma

Writing—original draft: Lu Zeng, Wentao Xu

Writing—review & editing: Jing Ai, Lu Zeng, Yang Qu, Xiaobin An

Ethics approval and consent to participate

All animal procedures were approved by the Institutional Animal Care and Use Committee at Harbin Medical University (no. HMUIRB-2008-06) and the Institute of Laboratory Animal Science of China (A5655-01). All procedures conformed to Directive 2010/63/EU of the European Parliament.

Consent for publication

Not applicable.

Availability of data

Data are available from the corresponding author upon reasonable request.

References

- Garre-Olmo J. Epidemiology of Alzheimer's disease and other dementias. *Rev Neurol*. 2018;66(11):377-386.
- Uddin MS, Mamun AA, Takeda S, Sarwar S, Begum M. Analyzing the chance of developing dementia among geriatric people: A cross-sectional pilot study in Bangladesh. *Psychogeriatrics*. 2019;19(2):87-94.
doi: 10.1111/psyg.12368
- Hebert LE, Weuve J, Scherr PA, Evans DA. Alzheimer disease in the United States (2010-2050) estimated using the 2010 census. *Neurology*. 2013;80(19):1778-1783.
doi: 10.1212/WNL.0b013e31828726f5
- Hojo Y, Murakami G, Mukai H, *et al*. Estrogen synthesis in the brain--role in synaptic plasticity and memory. *Mol Cell Endocrinol*. 2008;290(1-2):31-43.
doi: 10.1016/j.mce.2008.04.017
- Mosconi L, Rahman A. Increased Alzheimer's risk during the menopause transition: A 3-year longitudinal brain imaging study. *PLoS One*. 2018;13(12):e0207885.
doi: 10.1371/journal.pone.0207885
- Dumas JA, Kutz AM, Naylor MR, Johnson JV, Newhouse PA. Increased memory load-related frontal activation after estradiol treatment in postmenopausal women. *Horm Behav*. 2010;58(5):929-935.
doi: 10.1016/j.yhbeh.2010.09.003
- Kohama SG, Renner L, Landauer N, *et al*. Effect of ovarian hormone therapy on cognition in the aged female rhesus macaque. *J Neurosci*. 2016;36(40):10416-10424.
doi: 10.1523/JNEUROSCI.0909-16.2016
- Hao J, Rapp PR, Janssen WGM, *et al*. Interactive effects of age and estrogen on cognition and pyramidal neurons in monkey prefrontal cortex. *Proc Natl Acad Sci U S A*. 2007;104(27):11465-11470.
doi: 10.1073/pnas.0704757104
- Henderson VW. Alzheimer's disease: Review of hormone therapy trials and implications for treatment and prevention after menopause. *J Steroid Biochem Mol Biol*. 2014;142:99-106.
doi: 10.1016/j.jsbmb.2013.05.010
- Baxter MG, Roberts MT, Gee NA, Lasley BL, Morrison JH, Rapp PR. Multiple clinically relevant hormone therapy regimens fail to improve cognitive function in aged ovariectomized rhesus monkeys. *Neurobiol Aging*. 2013;34(7):1882-1890.
doi: 10.1016/j.neurobiolaging.2012.12.017
- Gill SS, Seitz DP. Lifestyles and cognitive health: What older individuals can do to optimize cognitive outcomes. *JAMA*. 2015;314(8):774-775.
doi: 10.1001/jama.2015.9526
- Bach-Faig A, Berry EM, Lairon D, *et al*. Mediterranean diet pyramid today. Science and cultural updates. *Public Health Nutr*. 2011;14(12a):2274-2284.
doi: 10.1017/s1368980011002515
- Lourida I, Soni M, Thompson-Coon J, *et al*. Mediterranean diet, cognitive function, and dementia: A systematic review. *Epidemiology*. 2013;24(4):479-489.
doi: 10.1097/EDE.0b013e3182944410
- Morris MC, Tangney CC, Wang Y, Sacks FM, Bennett DA, Aggarwal NT. MIND diet associated with reduced incidence of Alzheimer's disease. *Alzheimers Dement*. 2015;11(9):1007-1014.
doi: 10.1016/j.jalz.2014.11.009
- Omar SH. Mediterranean and MIND Diets containing olive biophenols reduces the prevalence of Alzheimer's disease. *Int J Mol Sci*. 2019;20(11):2797.
doi: 10.3390/ijms20112797
- Gardener SL, Rainey-Smith SR, Barnes MB, *et al*. Dietary patterns and cognitive decline in an Australian study of ageing. *Mol Psychiatry*. 2015;20(7):860-866.
doi: 10.1038/mp.2014.79
- Shakersain B, Santoni G, Larsson SC, *et al*. Prudent diet may attenuate the adverse effects of Western diet on cognitive decline. *Alzheimers Dement*. 2016;12(2):100-109.
doi: 10.1016/j.jalz.2015.08.002
- Kim Y, Koh I, Rho M. Deciphering the human microbiome using next-generation sequencing data and bioinformatics approaches. *Methods*. 2015;79-80:52-59.
doi: 10.1016/j.ymeth.2014.10.022
- Wang WL, Xu SY, Ren ZG, Tao L, Jiang JW, Zheng SS. Application of metagenomics in the human gut microbiome. *World J Gastroenterol*. 2015;21(3):803-814.
doi: 10.3748/wjg.v21.i3.803

20. Long-Smith C, O’Riordan KJ, Clarke G, Stanton C, Dinan TG, Cryan JF. Microbiota-gut-brain axis: New therapeutic opportunities. *Annu Rev Pharmacol Toxicol.* 2020;60:477-502.
doi: 10.1146/annurev-pharmtox-010919-023628
21. Morais LH, Schreiber HL 4th, Mazmanian SK. The gut microbiota-brain axis in behaviour and brain disorders. *Nat Rev Microbiol.* 2021;19(4):241-255.
doi: 10.1038/s41579-020-00460-0
22. Zmora N, Suez J, Elinav E. You are what you eat: Diet, health and the gut microbiota. *Nat Rev Gastroenterol Hepatol.* 2019;16(1):35-56.
doi: 10.1038/s41575-018-0061-2
23. Amar J, Burcelin R, Ruidavets JB, *et al.* Energy intake is associated with endotoxemia in apparently healthy men. *Am J Clin Nutr.* 2008;87(5):1219-1223.
doi: 10.1093/ajcn/87.5.1219
24. Cani PD, Amar J, Iglesias MA, *et al.* Metabolic endotoxemia initiates obesity and insulin resistance. *Diabetes.* 2007;56(7):1761-1772.
doi: 10.2337/db06-1491
25. Caesar R, Tremaroli V, Kovatcheva-Datchary P, Cani PD, Bäckhed F. Crosstalk between gut microbiota and dietary lipids aggravates WAT inflammation through TLR signaling. *Cell Metab.* 2015;22(4):658-668.
doi: 10.1016/j.cmet.2015.07.026
26. Pitts MW. Barnes maze procedure for spatial learning and memory in mice. *Bio Protoc.* 2018;8(5):e2744.
doi: 10.21769/bioprotoc.2744
27. Tanila H, Sipilä P, Shapiro M, Eichenbaum H. Brain aging: Impaired coding of novel environmental cues. *J Neurosci.* 1997;17(13):5167-5174.
doi: 10.1523/jneurosci.17-13-05167.1997
28. Leger M, Quiedeville A, Bouet V, *et al.* Object recognition test in mice. *Nat Protoc.* 2013;8(12):2531-2537.
doi: 10.1038/nprot.2013.155
29. Zhu H, Wang N, Yao L, *et al.* Moderate UV exposure enhances learning and memory by promoting a novel glutamate biosynthetic pathway in the brain. *Cell.* 2018;173(7):1716-1727.e17.
doi: 10.1016/j.cell.2018.04.014
30. Zhang S, Zeng L, Ma J, *et al.* Gut prevotellaceae-GABAergic septohippocampal pathway mediates spatial memory impairment in high-fat diet-fed ovariectomized mice. *Neurobiol Dis.* 2023;177:105993.
doi: 10.1016/j.nbd.2023.105993
31. Li Y, Cheng Y, Zhou Y, *et al.* High fat diet-induced obesity leads to depressive and anxiety-like behaviors in mice via AMPK/mTOR-mediated autophagy. *Exp Neurol.* 2022;348:113949.
doi: 10.1016/j.expneurol.2021.113949
32. Ding N, Zhang X, Zhang XD, *et al.* Impairment of spermatogenesis and sperm motility by the high-fat diet-induced dysbiosis of gut microbes. *Gut.* 2020;69(9):1608-1619.
doi: 10.1136/gutjnl-2019-319127
33. Sun P, Wang M, Li Z, *et al.* Eucommiae cortex polysaccharides mitigate obesogenic diet-induced cognitive and social dysfunction via modulation of gut microbiota and tryptophan metabolism. *Theranostics.* 2022;12(8):3637-3655.
doi: 10.7150/thno.72756
34. Edgar RC. UPARSE: Highly accurate OTU sequences from microbial amplicon reads. *Nat Methods.* 2013;10(10):996-998.
doi: 10.1038/nmeth.2604
35. Thackray VG. Sex, microbes, and polycystic ovary syndrome. *Trends Endocrinol Metab.* 2019;30(1):54-65.
doi: 10.1016/j.tem.2018.11.001
36. Arumugam M, Raes J, Pelletier E, *et al.* Enterotypes of the human gut microbiome. *Nature.* 2011;473(7346):174-180.
doi: 10.1038/nature09944
37. Dalile B, Kim C, Challinor A, *et al.* The EAT-Lancet reference diet and cognitive function across the life course. *Lancet Planet Health.* 2022;6(9):e749-e759.
doi: 10.1016/s2542-5196(22)00123-1
38. Beam CR, Kaneshiro C, Jang JY, Reynolds CA, Pedersen NL, Gatz M. Differences between women and men in incidence rates of dementia and Alzheimer’s disease. *J Alzheimers Dis.* 2018;64(4):1077-1083.
doi: 10.3233/jad-180141
39. Scheyer O, Rahman A, Hristov H, *et al.* Female sex and Alzheimer’s risk: The menopause connection. *J Prev Alzheimers Dis.* 2018;5(4):225-230.
doi: 10.14283/jpad.2018.34
40. Zhang S, An X, Huang S, *et al.* AhR/miR-23a-3p/PKC α axis contributes to memory deficits in ovariectomized and normal aging female mice. *Mol Ther Nucleic Acids.* 2021;24:79-91.
doi: 10.1016/j.omtn.2021.02.015
41. Gannon OJ, Robison LS, Salinero AE, *et al.* High-fat diet exacerbates cognitive decline in mouse models of Alzheimer’s disease and mixed dementia in a sex-dependent manner. 2022;19(1):110.
doi: 10.1186/s12974-022-02466-2
42. Al-Azzawi F, Palacios S. Hormonal changes during menopause. *Maturitas.* 2009;63(2):135-137.
doi: 10.1016/j.maturitas.2009.03.009

43. Lobo RA. Androgens in postmenopausal women: Production, possible role, and replacement options. *Obstet Gynecol Surv.* 2001;56(6):361-376.
doi: 10.1097/00006254-200106000-00022
44. Sah SK, Lee C, Jang JH, Park GH. Effect of high-fat diet on cognitive impairment in triple-transgenic mice model of Alzheimer's disease. *Biochem Biophys Res Commun.* 2017;493(1):731-736.
doi: 10.1016/j.bbrc.2017.08.122
45. Szablewski L. Human gut microbiota in health and Alzheimer's disease. *J Alzheimers Dis.* 2018;62(2):549-560.
doi: 10.3233/jad-170908
46. Pan W, Zhao J, Wu J, *et al.* Dimethyl itaconate ameliorates cognitive impairment induced by a high-fat diet via the gut-brain axis in mice. *Microbiome.* 2023;11(1):30.
doi: 10.1186/s40168-023-01471-8
47. Hooper LV, Midtvedt T, Gordon JI. How host-microbial interactions shape the nutrient environment of the mammalian intestine. *Annu Rev Nutr.* 2002;22:283-307.
doi: 10.1146/annurev.nutr.22.011602.092259
48. Gorvitovskaia A, Holmes SP, Huse SM. Interpreting *Prevotella* and *Bacteroides* as biomarkers of diet and lifestyle. *Microbiome.* 2016;4:15.
doi: 10.1186/s40168-016-0160-7
49. David LA, Maurice CF, Carmody RN, *et al.* Diet rapidly and reproducibly alters the human gut microbiome. *Nature.* 2014;505(7484):559-563.
doi: 10.1038/nature12820
50. Xue C, Li G, Zheng Q, *et al.* Tryptophan metabolism in health and disease. *Cell Metab.* 2023;35(8):1304-1326.
doi: 10.1016/j.cmet.2023.06.004
51. Mauvais-Jarvis F, Clegg DJ, Hevener AL. The role of estrogens in control of energy balance and glucose homeostasis. *Endocr Rev.* 2013;34(3):309-338.
doi: 10.1210/er.2012-1055